# POTENTIAL FLOW OF A SECOND-ORDER FLUID OVER A TRI-AXIAL ELLIPSOID

F. VIANA, T. FUNADA, D. D. JOSEPH, N. TASHIRO, AND Y. SONODA

The problem of potential flow of a second-order fluid around an ellipsoid is solved, and the flow and stress fields are computed. The flow fields are determined by the harmonic potential but the stress fields depend on viscosity and the parameters of the second-order fluid. The stress fields on the surface of a tri-axial ellipsoid depend strongly on the ratios of principal axes and are such as to suggest the formation of gas bubble with a round flat nose and two-dimensional cusped trailing edge. A thin flat trailing edge gives rise to a large stress which makes the thin trailing edge thinner.

## 1. Introduction

Wang and Joseph [15] studied the potential flow of a second-order fluid over a sphere or an ellipse. The potential for the ellipse is a classical solution given as a complex function of a complex variable. The stress for a second-order fluid was evaluated on this irrotational flow. An important result of this study is that the normal stress at a point of stagnation changes from compression to tension strongly under even mild conditions on the viscoelastic parameters.

Here, we extend the three dimensional study of Wang and Joseph [15] to the case of flow over an ellipsoid whose three principal axes may be unequal. The solution of Laplace's equation ($\nabla^2\phi = 0$) bounded internally by an ellipsoid

$$\frac{x^2}{a^2} + \frac{y^2}{b^2} + \frac{z^2}{c^2} = 1, \tag{1.1}$$

moving with constant velocity $U$ in the direction $x$ is given by Lamb [10, page 152] and Milne-Thomson [12, pages 510–512]. Since $a$ is arbitrary their solution is readily adapted to the case of a translating ellipsoid in any of the three principal directions. To be definite we adopt the convention that

$$a > b > c. \tag{1.2}$$

The motion of an ellipsoid in an arbitrary direction may be formed from superposing of motions in three principal directions.

Here we compute solutions relative to a stationary ellipsoid in a uniform stream. Since our goal is the calculation of irrotational viscous and non-Newtonian (second-order) stresses we must compute working formulas, not in the literature, for velocities, pressure and the derivatives of velocity required to calculate stresses. We first use these formulas to compute the velocity field and pressure for the classical problem of irrotational flow of an inviscid fluid. Then we apply these same formulas to the case of a viscous, second-order, non-Newtonian fluid.

The main goal of our calculations for the second-order fluid model is to identify mechanisms which lead to "two-dimensional cusps" at the trailing edge of a gas bubble rising in an unbounded liquid where axisymmetric solutions might be expected. We calculate the effects of viscosity, second-order viscoelasticity and inertia. The effects of viscoelasticity are opposite to the effects of inertia; under modest and realizable assumptions about the values of the second-order fluid parameters, the normal stresses at points of stagnation change from compression to tension. The effect of inertia and elasticity are essentially symmetric in that they depend on squares of velocity and velocity gradients but the effects of viscosity are asymmetric.

For the rising gas bubbles, the effects of the second-order and viscous terms on the normal stress are such as to extend and flatten the trailing edge. These calculations suggest that "two-dimensional cusping" can be viewed as an instability in which a thin flat trailing edge gives rise to a large stress which makes the thin trailing edge even thinner.

This paper is organized as follows: in Section 2, we review the physics at the trailing edge of a rising gas bubble. In Section 3, we transform general expressions in the literature for flow around a triaxial ellipsoid into a form suitable for calculation. In Section 4, we give expressions for the stresses in a second order fluid model evaluated on the irrotational flow; the formulas for the flow field are given in Section 5. The normal stress distribution on the ellipsoid is computed in Section 6.

## 2. Fluid mechanics of two-dimensional cusping at the trailing edge of gas bubbles rising in viscoelastic liquids

An air bubble rising freely in a non-Newtonian liquid tends to be prolate and can develop a cusp at the trailing edge as shown in Figure 2.1a. This cuspidal tale occurs only in gas bubbles rising freely in non-Newtonian liquids. Joseph et al. [8] defined the cuspidal tails as point singularities of curvature. They also stated that the build-up of extensional stresses near stagnation points may favor the formation of cusps.

In its analysis of cusped interfaces, Joseph [5] suggests that the strong tendency for cusping in non-Newtonian fluids is a mechanism for eliminating stagnation points for the relaxation of elongational stresses.

Hassager [2] was the first to show that the cusp was not rotationally symmetric but two-dimensional, with a broad shape in one view and so flat that exhibits a point cusp when observed orthogonally. Liu et al. [11] presented new experimental evidence of the two-dimensional characteristic of cusped bubbles (see Figure 2.1). They also reported the different shapes of the broad edge observed in experiments.
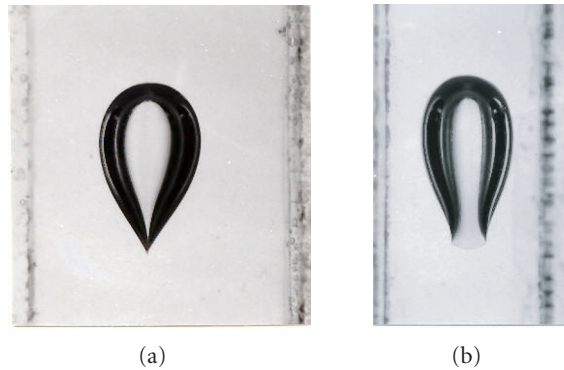
<div align="center">(a)                                    (b)</div>

Figure 2.1. Two orthogonal views showing the (a) cusped and (b) broad shape of the trailing edge of an air bubble ($2\,\text{cm}^3$), rising in a viscoelastic liquid (S1). The two photographs are from Liu et al. [11].

A comprehensive review of the literature concerning bubbles rising in non-Newtonian fluids and the analysis of two-dimensional cusps at the trailing edge of the bubbles can be found in Liu et al. [11]. From their experimental results for air bubbles of different sizes rising in various viscoelastic liquids and in columns of different configurations, they concluded that the formation of cusps is independent of the size and shape of the column.

Liu et al. [11] reported that the cusping tails occur at the trailing edge of a bubble rising in a non-Newtonian liquid for capillary numbers (Ca) of 1 or higher.

Pillapakkam and Singh [13] developed a code to simulate the deformation of a gas bubble rising in an Oldroyd-B liquid. They found that the shape of the bubble depends on both the Capillary (Ca) and Deborah (De) numbers. They observed that in general, the gas bubble assumes an elongated shape with the frontal part round and when both Ca and De numbers are of the order of 1 a two-dimensional cusp is developed at the trailing edge. They claim to show that the pull out effects of sufficiently large viscoelastic stresses near the trailing edge of the bubble cause the formation of a cuspidal tail.

An interesting aspect of the rise of gas bubbles in a viscoelastic liquid is that the fluid in the region behind the bubble moves in the opposite direction of the bubble. This phenomenon was reported for the first time by Hassager [2] and was termed "negative wake."

Pillapakkam and Singh [14] presented some numerical results that indicate a negative wake in the region behind gas bubbles rising in viscoelastic liquids. They associated the presence of a negative wake with a certain range of two viscoelastic parameters, the Deborah number and the polymer concentration. They found that for a polymer concentration of 2, the shape of the fore part of the bubble is round and no negative wake is observed. For polymer concentrations higher than 2, they reported the existence of a negative wake in the region behind the bubble.

Here we show that the normal stress distribution at the surface of the bubble may cause the formation of a cusp at the trailing edge. We analyze the effect of the normal stress on the shape of a gas bubble by computing the normal stress at the surface of a tri-axial ellipsoid immersed in a uniform irrotational flow of a second-order fluid.

## 3. Irrotational flow of an incompressible and inviscid fluid over a stationary ellipsoid

The flows for which the vorticity vector vanishes ($\boldsymbol{\omega} = \nabla \times \mathbf{u}$) everywhere in the flow field are said to be irrotational. Since for any scalar function $\phi$ it is satisfied that $\nabla \times \nabla \phi = 0$, the condition of irrotationality is redefined by choosing $\mathbf{u} = \nabla \phi$. In which case the function $\phi$ is called the velocity potential. By using the continuity equation of an incompressible fluid ($\nabla \cdot \mathbf{u} = 0$) gives the Laplace's equation ($\nabla^2 \phi = 0$).

In this section, we present the velocity potential for the flow induced by an ellipsoid that translates along the $x$-axis given by Lamb [10] and Milne-Thomson [12]. In addition, we compute the velocity components and the inviscid pressure for the irrotational flow around a stationary ellipsoid.

The harmonic function presented by Lamb [10] represents the solution to the Laplace's equation expressed in terms of a special system of orthogonal curvilinear coordinates known as ellipsoidal coordinates.

The equation

$$\frac{x^2}{a^2 + \theta} + \frac{y^2}{b^2 + \theta} + \frac{z^2}{c^2 + \theta} = 1 \quad a > b > c, \tag{3.1}$$

where $a, b, c$ are fixed and $\theta$ is a parameter, represents for any constant value of $\theta$ a central quadric of a confocal system. In particular, when $\theta = 0$, we have the ellipsoid given by (1.1).

Equation (3.1) leads to the expression

$$\begin{aligned} f(\theta) = &\; x^2 (b^2 + \theta)(c^2 + \theta) + y^2 (c^2 + \theta)(a^2 + \theta) \\ &+ z^2 (a^2 + \theta)(b^2 + \theta) - (a^2 + \theta)(b^2 + \theta)(c^2 + \theta) = 0 \end{aligned} \tag{3.2}$$

which is a cubic equation in $\theta$ and has three roots, say $\lambda$, $\mu$, and $\nu$, that are distributed as follows (see Kellogg [9]):

$$-a^2 \leq \nu \leq -b^2 \leq \mu \leq -c^2 \leq \lambda. \tag{3.3}$$

The values of $x$, $y$, $z$ can be expressed as functions of $\lambda$, $\mu$, and $\nu$ by the following equations,

$$\begin{aligned} x^2 &= \frac{(a^2 + \lambda)(a^2 + \mu)(a^2 + \nu)}{(a^2 - b^2)(a^2 - c^2)}, \\ y^2 &= \frac{(b^2 + \lambda)(b^2 + \mu)(b^2 + \nu)}{(b^2 - c^2)(b^2 - a^2)}, \\ z^2 &= \frac{(c^2 + \lambda)(c^2 + \mu)(c^2 + \nu)}{(c^2 - a^2)(c^2 - b^2)}. \end{aligned} \tag{3.4}$$

It follows that

$$\frac{\partial x}{\partial \lambda} = \frac{1}{2}\frac{x}{a^2+\lambda}, \qquad \frac{\partial y}{\partial \lambda} = \frac{1}{2}\frac{y}{b^2+\lambda}, \qquad \frac{\partial z}{\partial \lambda} = \frac{1}{2}\frac{z}{c^2+\lambda}, \tag{3.5}$$

and hence

$$h_1^2 = \frac{1}{4}\left(\frac{x^2}{(a^2+\lambda)^2} + \frac{y^2}{(b^2+\lambda)^2} + \frac{z^2}{(c^2+\lambda)^2}\right). \tag{3.6}$$

The square of the scale factors $h_1$, $h_2$, $h_3$ in ellipsoidal coordinates are given by

$$h_1^2 = \frac{1}{4}\frac{(\lambda-\mu)(\lambda-\nu)}{(a^2+\lambda)(b^2+\lambda)(c^2+\lambda)},$$

$$h_2^2 = \frac{1}{4}\frac{(\mu-\nu)(\mu-\lambda)}{(a^2+\mu)(b^2+\mu)(c^2+\mu)}, \tag{3.7}$$

$$h_3^2 = \frac{1}{4}\frac{(\nu-\lambda)(\nu-\mu)}{(a^2+\nu)(b^2+\nu)(c^2+\nu)}.$$

The direction-cosines of the outward normal to the three surfaces which pass through $(x,y,z)$ will be

$$\left(\frac{1}{h_1}\frac{\partial x}{\partial \lambda}, \frac{1}{h_1}\frac{\partial y}{\partial \lambda}, \frac{1}{h_1}\frac{\partial z}{\partial \lambda}\right), \qquad \left(\frac{1}{h_2}\frac{\partial x}{\partial \mu}, \frac{1}{h_2}\frac{\partial y}{\partial \mu}, \frac{1}{h_2}\frac{\partial z}{\partial \mu}\right), \qquad \left(\frac{1}{h_3}\frac{\partial x}{\partial \nu}, \frac{1}{h_3}\frac{\partial y}{\partial \nu}, \frac{1}{h_3}\frac{\partial z}{\partial \nu}\right). \tag{3.8}$$

We may note that if $\lambda$, $\mu$, $\nu$ be regarded as functions of $x$, $y$, $z$ the direction-cosines of the three line-elements above considered can also be expressed in the forms

$$\left(h_1\frac{\partial \lambda}{\partial x}, h_1\frac{\partial \lambda}{\partial y}, h_1\frac{\partial \lambda}{\partial z}\right), \qquad \left(h_2\frac{\partial \mu}{\partial x}, h_2\frac{\partial \mu}{\partial y}, h_2\frac{\partial \mu}{\partial z}\right), \qquad \left(h_3\frac{\partial \nu}{\partial x}, h_3\frac{\partial \nu}{\partial y}, h_3\frac{\partial \nu}{\partial z}\right), \tag{3.9}$$

from which, and from (3.8), various interesting relations can be inferred. For our present purpose the following relations would be useful,

$$\frac{\partial \lambda}{\partial x} = \frac{1}{h_1^2}\frac{\partial x}{\partial \lambda} = \frac{x}{2h_1^2(a^2+\lambda)},$$

$$\frac{\partial \lambda}{\partial y} = \frac{1}{h_1^2}\frac{\partial y}{\partial \lambda} = \frac{y}{2h_1^2(b^2+\lambda)}, \tag{3.10}$$

$$\frac{\partial \lambda}{\partial z} = \frac{1}{h_1^2}\frac{\partial z}{\partial \lambda} = \frac{z}{2h_1^2(c^2+\lambda)}.$$

The Laplacian ($\nabla^2$) of the scalar function $\phi$ in ellipsoidal coordinates can be written in the form

$$\nabla^2\phi = \frac{1}{h_1 h_2 h_3}\left\{\frac{\partial}{\partial\lambda}\left(\frac{h_2 h_3}{h_1}\frac{\partial\phi}{\partial\lambda}\right) + \frac{\partial}{\partial\mu}\left(\frac{h_3 h_1}{h_2}\frac{\partial\phi}{\partial\mu}\right) + \frac{\partial}{\partial\nu}\left(\frac{h_1 h_2}{h_3}\frac{\partial\phi}{\partial\nu}\right)\right\}. \tag{3.11}$$

Equating this to zero, we obtain the Laplace's equation that is the general expression of continuity given in ellipsoidal coordinates.

Solutions to this equation are called ellipsoidal harmonics. From Milne-Thomson [12] and Lamb [10], the corresponding ellipsoidal harmonics are given by

$$\phi_x = Cx\int_\lambda^\infty \frac{d\lambda}{(a^2+\lambda)\sqrt{(a^2+\lambda)(b^2+\lambda)(c^2+\lambda)}}, \tag{3.12}$$

$$\phi_{yz} = Cyz\int_\lambda^\infty \frac{d\lambda}{(b^2+\lambda)(c^2+\lambda)\sqrt{(a^2+\lambda)(b^2+\lambda)(c^2+\lambda)}}, \tag{3.13}$$

where $C$ is an arbitrary constant, and $x$, $y$, $z$ are supposed expressed in terms of $\lambda$, $\mu$, $\nu$ by means of (3.4).

For a full account of the solution of Laplace's equation in ellipsoidal coordinates we must refer to Lamb [10] and Milne-Thomson [12].

For the ellipsoid given by (1.1), which corresponds to $\lambda = 0$, moving in the direction of the $x$-axis with velocity $U$, the boundary condition is

$$-\frac{\partial\phi}{\partial n} = U\cos\theta_x \quad \text{or} \quad \frac{\partial\phi}{\partial\lambda} = -U\frac{\partial x}{\partial\lambda}, \quad \lambda = 0. \tag{3.14}$$

Thus when $\lambda = 0$, $\phi = -Ux$, and when $\lambda \to \infty$, $\phi \to 0$. These conditions are satisfied by the function $\phi_x$ of (3.12).

Applying the boundary conditions to (3.12) gives

$$C = \frac{abcU}{2-\alpha_0}, \tag{3.15}$$

where

$$\alpha_0 = abc\int_0^\infty \frac{d\lambda}{(a^2+\lambda)\sqrt{(a^2+\lambda)(b^2+\lambda)(c^2+\lambda)}}. \tag{3.16}$$

The constant $\alpha_0$ depends solely on the semiaxes $a$, $b$, $c$ of the ellipsoid. Its numerical evaluation requires the use of elliptic integrals.

Thus, finally,

$$\phi = \frac{abcUx}{2 - \alpha_0} \int_\lambda^\infty \frac{d\lambda}{(a^2 + \lambda)^{3/2} (b^2 + \lambda)^{1/2} (c^2 + \lambda)^{1/2}}, \tag{3.17}$$

and on the surface of the ellipsoid we have, from (3.12) with $\lambda = 0$,

$$\phi = \frac{x\alpha_0 U}{2 - \alpha_0}. \tag{3.18}$$

Equation (3.17) represents the potential for the space external to the ellipsoid (1.1) that moves with velocity $U$ in a liquid at rest at infinity. This result corresponds to an origin moving with the ellipsoid. By superposing a uniform flow with velocity $U$, in the positive direction of the $x$-axis, giving

$$\phi = xU \left[ \frac{abc}{2 - \alpha_0} \int_\lambda^\infty \frac{d\lambda}{(a^2 + \lambda) \sqrt{(a^2 + \lambda)(b^2 + \lambda)(c^2 + \lambda)}} + 1 \right] \tag{3.19}$$

and defining

$$\Gamma = U \left[ \frac{abc}{2 - \alpha_0} \int_\lambda^\infty \frac{d\lambda}{(a^2 + \lambda) \sqrt{(a^2 + \lambda)(b^2 + \lambda)(c^2 + \lambda)}} + 1 \right], \tag{3.20}$$

it follows that

$$\phi = x\Gamma, \tag{3.21}$$

where $\Gamma$ is a function of $\lambda$ only.

Equation (3.21) represents the velocity potential for the flow around a stationary ellipsoid.

The function $\Gamma$ given by (3.20) involves the elliptic integral,

$$I = \int_\lambda^\infty \frac{d\lambda}{(a^2 + \lambda) \sqrt{(a^2 + \lambda)(b^2 + \lambda)(c^2 + \lambda)}}. \tag{3.22}$$

The solution to this integral, obtained from the handbook of elliptic integrals written by Byrd and Friedman [1, page 5], is given by

$$I = \frac{2[F(\varphi,k) - E(\varphi,k)]}{k^2(a^2 - c^2)\sqrt{a^2 - c^2}}, \tag{3.23}$$

where

$$\varphi = \arcsin\sqrt{\frac{a^2 - c^2}{\lambda + a^2}},$$

$$k = \sqrt{\frac{a^2 - b^2}{a^2 - c^2}} \tag{3.24}$$

and the functions $F(\varphi,k)$ and $E(\varphi,k)$ represent the incomplete elliptic integral of the first kind and the Legendre's incomplete elliptic integral of the second kind, respectively. The values of the functions $F(\varphi,k)$ and $E(\varphi,k)$ are tabulated in Byrd and Friedman [1] for given values of $\varphi$ and $k$.

The differentiation of the elliptic functions $F(\varphi,k)$ and $E(\varphi,k)$ with respect to $\varphi$ yields (see Byrd and Friedman [1, page 284])

$$\frac{d}{d\varphi}F(\varphi,k) = \frac{1}{\sqrt{1 - k^2\sin^2\varphi}},$$

$$\frac{d}{d\varphi}E(\varphi,k) = \sqrt{1 - k^2\sin^2\varphi}. \tag{3.25}$$

With the expression for the elliptic integral given by (3.23), (3.20) becomes

$$\Gamma = U\left[\frac{abc}{2 - \alpha_0}\frac{2[F(\varphi,k) - E(\varphi,k)]}{(a^2 - b^2)\sqrt{a^2 - c^2}} + 1\right]. \tag{3.26}$$

For an irrotational flow the velocity components are given by

$$\mathbf{u} = \nabla\phi = \frac{\partial\phi}{\partial x_i}. \tag{3.27}$$

Applying (3.27) to the scalar function given by (3.21) gives

$$u = \frac{\partial(x\Gamma)}{\partial x} = \Gamma + x\frac{\partial\Gamma}{\partial\lambda}\frac{\partial\lambda}{\partial x} = \Gamma + \frac{x^2}{2h_1^2(a^2 + \lambda)}\frac{\partial\Gamma}{\partial\lambda},$$

$$v = \frac{\partial(x\Gamma)}{\partial y} = x\frac{\partial\Gamma}{\partial\lambda}\frac{\partial\lambda}{\partial y} = \frac{xy}{2h_1^2(b^2 + \lambda)}\frac{\partial\Gamma}{\partial\lambda},$$

$$w = \frac{\partial(x\Gamma)}{\partial z} = x\frac{\partial\Gamma}{\partial\lambda}\frac{\partial\lambda}{\partial z} = \frac{xz}{2h_1^2(c^2 + \lambda)}\frac{\partial\Gamma}{\partial\lambda}, \tag{3.28}$$
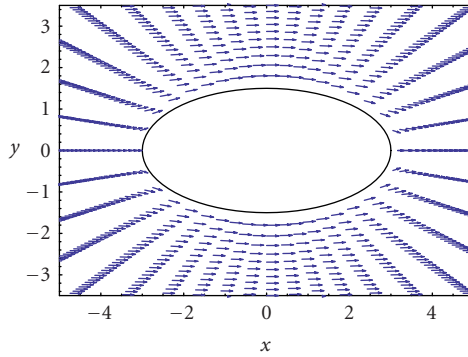
Figure 3.1. Velocity field of an irrotational, inviscid flow around an ellipsoid with semiaxes $a = 3$, $b = 1.5$, $c = 0.75$, and a Reynolds number of 0.05. Two-dimensional representation of the velocity field at the centerline of the ellipsoid ($z = 0$).

which represent the velocity components of the irrotational flow of an inviscid fluid around an ellipsoid.

It is pertinent to introduce at this point, the first, second, and third derivatives of $\Gamma$ that would be used in determining the velocity components and their derivatives:

$$\frac{\partial \Gamma}{\partial \lambda} = -\frac{abcU}{(2 - \alpha_0)(a^2 + \lambda)^{3/2}(b^2 + \lambda)^{1/2}(c^2 + \lambda)^{1/2}},$$

$$\frac{\partial^2 \Gamma}{\partial \lambda^2} = -\frac{\partial \Gamma}{\partial \lambda}\left[\frac{3}{2(a^2 + \lambda)} + \frac{1}{2(b^2 + \lambda)} + \frac{1}{2(c^2 + \lambda)}\right],$$

$$\frac{\partial^3 \Gamma}{\partial \lambda^3} = \frac{\partial \Gamma}{\partial \lambda}\left[\frac{3}{2(a^2 + \lambda)} + \frac{1}{2(b^2 + \lambda)} + \frac{1}{2(c^2 + \lambda)}\right]^2$$

$$+ \frac{\partial \Gamma}{\partial \lambda}\left[\frac{3}{2(a^2 + \lambda)^2} + \frac{1}{2(b^2 + \lambda)^2} + \frac{1}{2(c^2 + \lambda)^2}\right].$$

$$(3.29)$$

A two-dimensional representation of the flow field at the centerline of a tri-axial ellipsoid is shown in Figure 3.1. This representation corresponds to a tri-axial ellipsoid with semiaxes $a/b = b/c = 2$ and a Reynolds number of 0.05.

Integration of the Euler's equation yields the Bernoulli equation. Thus, for an incompressible, irrotational and steady flow the inviscid pressure equation can be written as

$$p_I = \frac{\rho}{2}\left(U^2 - |\nabla\phi|^2\right) + p_\infty, \tag{3.30}$$

where $U$ and $p_\infty$ are the velocity and the pressure far away from the flow field.

Introducing the expression for the magnitude of the velocity vector in (3.30) yields

$$p_I = \frac{\rho}{2}\left[U^2 - \Gamma^2 - \frac{x^2}{h_1^2}\left(\frac{\Gamma}{(a^2 + \lambda)} + d\Gamma_\lambda\right)d\Gamma_\lambda\right] + p_\infty. \tag{3.31}$$
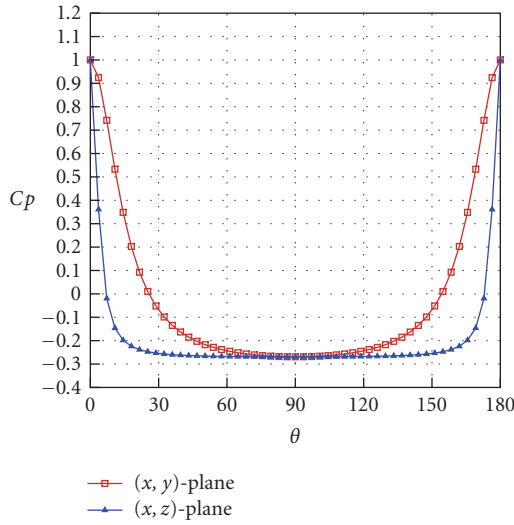
Figure 3.2. Pressure coefficient distribution on the surface of an ellipsoid for two cross sections in the $(x, y)$- and $(x, z)$-planes with $z = 0$ and $y = 0$, respectively.

At the surface of the ellipsoid ($\lambda = 0$) the pressure distribution can be obtained by evaluating the following expression,

$$p_{Is} = \frac{\rho U^2}{2(2 - \alpha_0)^2} \left[ \alpha_0 (\alpha_0 - 4) + \frac{4x^2 b^4 c^4}{(x^2 b^4 c^4 + y^2 a^4 c^4 + z^2 a^4 b^4)} \right] + p_\infty. \tag{3.32}$$

The nondimensional pressure on the surface of the ellipsoid is obtained by substituting (3.32) into the pressure coefficient defined as

$$C_p \equiv \frac{p - p_\infty}{(1/2)\rho U^2}. \tag{3.33}$$

A plot of this function in the $(x, y)$- and $(x, z)$-planes is given in **Figure 3.2**. It shows a symmetric pressure distribution over the ellipsoid. At the fore and rear stagnation points the pressure force is maximum and $C_p = 1$. As we move around the ellipsoid, the fluid accelerates and the pressure drops accordingly. At $\theta = \pi/2$ the pressure has dropped to $C_p = -0.269$. The pressure drops faster in the $(x, z)$-plane where the cross section is flatter than in the $(x, y)$-plane due to the difference in curvature.

The velocity gradient can be decomposed into its symmetric and anti-symmetric parts. The symmetric part is associated with the straining motions while the anti-symmetric part indicates the rotational motion of a fluid element. Thus, the velocity gradient can be written as

$$\mathbf{L} = \nabla \mathbf{u} = \mathbf{D} + \boldsymbol{\Omega}, \tag{3.34}$$

where $\mathbf{D} = (1/2)(\nabla \mathbf{u} + \nabla \mathbf{u}^T)$ and $\boldsymbol{\Omega} = (1/2)(\nabla \mathbf{u} - \nabla \mathbf{u}^T)$, represent the strain or deformation and the rotation tensors, respectively.

Since the rotation tensor is directly proportional to the vorticity vector, for an irrotational flow field, the anti-symmetric part of the velocity gradient is identically zero. Thus, the strain tensor is equal to the velocity gradient tensor ($\mathbf{D} = \mathbf{L}$).

For the flow field given by (3.28) the components of the strain tensor are:

$$D_{ij} = L_{ij} = \frac{\partial u_j}{\partial x_i},$$

$$L_{11} = \frac{\partial u}{\partial x} = \left(2\frac{\partial \lambda}{\partial x} + x\frac{\partial^2 \lambda}{\partial x^2}\right)\frac{\partial \Gamma}{\partial \lambda} + x\left(\frac{\partial \lambda}{\partial x}\right)^2 \frac{\partial^2 \Gamma}{\partial \lambda^2},$$

$$L_{12} = \frac{\partial v}{\partial x} = \frac{\partial u}{\partial y} = \left(\frac{\partial \lambda}{\partial y} + x\frac{\partial^2 \lambda}{\partial x \partial y}\right)\frac{\partial \Gamma}{\partial \lambda} + x\left(\frac{\partial \lambda}{\partial x}\frac{\partial \lambda}{\partial y}\right)\frac{\partial^2 \Gamma}{\partial \lambda^2},$$

$$L_{13} = \frac{\partial w}{\partial x} = \frac{\partial u}{\partial z} = \left(\frac{\partial \lambda}{\partial z} + x\frac{\partial^2 \lambda}{\partial x \partial z}\right)\frac{\partial \Gamma}{\partial \lambda} + x\left(\frac{\partial \lambda}{\partial x}\frac{\partial \lambda}{\partial z}\right)\frac{\partial^2 \Gamma}{\partial \lambda^2}, \qquad (3.35)$$

$$L_{22} = \frac{\partial v}{\partial y} = x\frac{\partial^2 \lambda}{\partial y^2}\frac{\partial \Gamma}{\partial \lambda} + x\left(\frac{\partial \lambda}{\partial y}\right)^2 \frac{\partial^2 \Gamma}{\partial \lambda^2},$$

$$L_{23} = \frac{\partial w}{\partial y} = \frac{\partial v}{\partial z} = x\frac{\partial^2 \lambda}{\partial y \partial z}\frac{\partial \Gamma}{\partial \lambda} + x\left(\frac{\partial \lambda}{\partial y}\frac{\partial \lambda}{\partial z}\right)\frac{\partial^2 \Gamma}{\partial \lambda^2},$$

$$L_{33} = \frac{\partial w}{\partial z} = x\frac{\partial^2 \lambda}{\partial z^2}\frac{\partial \Gamma}{\partial \lambda} + x\left(\frac{\partial \lambda}{\partial z}\right)^2 \frac{\partial^2 \Gamma}{\partial \lambda^2}.$$

## 4. Second-order fluid model

For an incompressible fluid, the stress tensor can be written as

$$\mathbf{T} = -p\mathbf{I} + \mathbf{S}, \qquad (4.1)$$

where $p$ is pressure and $\mathbf{S}$ is the extra stress which is modeled by a constitutive equation. There is not a single constitutive equation for all flow motions. For very slow flows, all the models collapse into a single form, the second-order fluid.

A second-order fluid is an asymptotic approximation to the stress for nearly steady and very slow flow. It is quadratic in the shear rate and represents the recent memory of the fluid by a time derivative (Joseph [6]).

The approximation to $\mathbf{S}$ for a second-order fluid is given by (see Joseph [4])

$$\mathbf{S} = \eta\mathbf{A} + \alpha_1\mathbf{B} + \alpha_2\mathbf{A}^2, \qquad (4.2)$$

where $\mathbf{A} = \mathbf{L} + \mathbf{L}^T$, is twice the symmetric part of the velocity gradient $\mathbf{L}$, and

$$\mathbf{B} = \frac{\partial \mathbf{A}}{\partial t} + (\mathbf{u} \cdot \nabla)\mathbf{A} + \mathbf{AL} + \mathbf{L}^T\mathbf{A}. \qquad (4.3)$$

Thus, for a second-order fluid the stress tensor can be written as

$$\mathbf{T} = -p\mathbf{I} + \eta\mathbf{A} + \alpha_1\mathbf{B} + \alpha_2\mathbf{A}^2, \qquad (4.4)$$

where $\mathbf{A}$ and $\mathbf{B}$ are known as the first and second Rivlin-Ericksen tensors (see Joseph and Feng [7]).

The parameter $\eta$ is the zero-shear viscosity and the parameters $\alpha_1 = -n_1/2$ and $\alpha_2 = n_1 + n_2$, the quadratic constants, are related by $\hat{\beta} = 3\alpha_1 + 2\alpha_2 \geq 0$; where $n_1$ and $n_2$ are constants obtained from the first and second normal stress differences and $\hat{\beta}$ is the climbing constant.

After Joseph [4], the Bernoulli equation for potential flow of a second-order fluid and in particular for steady flow can be written as

$$p = \frac{\rho}{2}\left(U^2 - |\nabla\phi|^2\right) + \frac{\hat{\beta}}{4}\operatorname{tr}\mathbf{A}^2 + p_\infty. \tag{4.5}$$

By introducing the scalar function for the pressure given by (4.5) and the steady form of (4.3) into (4.4) and rearranging, we get

$$\mathbf{T} = -\left[\frac{\rho}{2}\left(U^2 - |\nabla\phi|^2\right) + \hat{\beta}\chi + p_\infty\right]\mathbf{I} + \eta\mathbf{A} + \alpha_1(\mathbf{u}\cdot\nabla)\mathbf{A} + (\alpha_1 + \alpha_2)\mathbf{A}^2. \tag{4.6}$$

In index notation we have

$$A_{ij} = 2\frac{\partial^2\phi}{\partial x_i \partial x_j} = 2\frac{\partial u_j}{\partial x_i},$$

$$\chi = \frac{1}{4}\operatorname{tr}\mathbf{A}^2 = \frac{\partial^2\phi}{\partial x_i \partial x_k}\frac{\partial^2\phi}{\partial x_k \partial x_i} = \frac{\partial u_k}{\partial x_i}\frac{\partial u_i}{\partial x_k} = \left(\frac{\partial u_k}{\partial x_i}\right)^2,$$

$$T_{ij} = -\left[\frac{\rho}{2}\left(U^2 - \left|\frac{\partial\phi}{\partial x_i}\right|^2\right) + \hat{\beta}\chi + p_\infty\right]\delta_{ij} + \eta A_{ij} + \alpha_1\frac{\partial\phi}{\partial x_k}\frac{\partial}{\partial x_k}A_{ij} + (\alpha_1 + \alpha_2)A_{ik}A_{kj}. \tag{4.7}$$

## 5. Irrotational flow of a second-order fluid over a stationary ellipsoid

The set of equations that fully define the irrotational and steady flow of a second-order fluid around an ellipsoid is given next,

$$\phi = x\Gamma(\lambda), \qquad \mathbf{u} = \nabla\phi, \qquad \nabla\cdot\mathbf{u} = 0,$$

$$\mathbf{T} = -p\mathbf{I} + \eta\mathbf{A} + \alpha_1(\mathbf{u}\cdot\nabla)\mathbf{A} + (\alpha_1 + \alpha_2)\mathbf{A}^2,$$

$$\rho(\mathbf{u}\cdot\nabla)\mathbf{u} = -\nabla p + \eta\nabla^2\mathbf{u} + \nabla\cdot\left[\alpha_1(\mathbf{u}\cdot\nabla)\mathbf{A} + (\alpha_1 + \alpha_2)\mathbf{A}^2\right],$$

$$p = \frac{\rho}{2}\left(U^2 - |\nabla\phi|^2\right) + \frac{\hat{\beta}}{4}\operatorname{tr}\mathbf{A}^2 + p_\infty, \tag{5.1}$$

$$\mathbf{A} = \mathbf{L} + \mathbf{L}^T = 2\frac{\partial^2\phi}{\partial x_i \partial x_j}, \qquad \frac{1}{4}\operatorname{tr}\mathbf{A}^2 = \frac{\partial^2\phi}{\partial x_i \partial x_k}\frac{\partial^2\phi}{\partial x_k \partial x_i}, \qquad (\mathbf{u}\cdot\nabla)\mathbf{A} = \frac{\partial\phi}{\partial x_k}\frac{\partial}{\partial x_k}A_{ij}.$$

The normal component of the stress is computed as

$$T_{nn} = \mathbf{n}\cdot\mathbf{T}\cdot\mathbf{n}, \tag{5.2}$$

where **n** is the unit vector normal to the surface of the ellipsoid (1.1) and is given by

$$\mathbf{n} = \left(\frac{x}{a^2}\mathbf{i} + \frac{y}{b^2}\mathbf{j} + \frac{z}{c^2}\mathbf{k}\right)\Bigg/\sqrt{\frac{x^2}{a^4} + \frac{y^2}{b^4} + \frac{z^2}{c^4}}. \tag{5.3}$$

The normal component of the stress tensor in index notation, in terms of the velocity components, is given by

$$T_{nn} = n_i n_j T_{ij} = -\left[\frac{\rho}{2}\left(U^2 - u_i u_i\right) + \hat{\beta}\chi + p_\infty\right] + 2\eta n_i n_j \frac{\partial u_j}{\partial x_i}$$
$$+ 2\alpha_1 n_i n_j u_k \frac{\partial^2 u_j}{\partial x_k \partial x_i} + 4(\alpha_1 + \alpha_2) n_i n_j \frac{\partial u_k}{\partial x_i}\frac{\partial u_j}{\partial x_k}. \tag{5.4}$$

Expanding (5.4) yields

$$T_{nn} = -\frac{\rho}{2}\left[U^2 - (u^2 + v^2 + w^2)\right] - p_\infty$$

$$- (3\alpha_1 + 2\alpha_2)\left[\left(\frac{\partial u}{\partial x}\right)^2 + \left(\frac{\partial v}{\partial y}\right)^2 + \left(\frac{\partial w}{\partial z}\right)^2 + 2\left(\frac{\partial v}{\partial x}\right)^2 + 2\left(\frac{\partial w}{\partial x}\right)^2 + 2\left(\frac{\partial w}{\partial y}\right)^2\right]$$

$$+ 2\eta\left[n_x^2\frac{\partial u}{\partial x} + n_y^2\frac{\partial v}{\partial y} + n_z^2\frac{\partial w}{\partial z} + 2n_x n_y\frac{\partial v}{\partial x} + 2n_x n_z\frac{\partial w}{\partial x} + 2n_y n_z\frac{\partial w}{\partial y}\right]$$

$$+ 2\alpha_1\left[n_x^2\left(u\frac{\partial^2 u}{\partial x^2} + v\frac{\partial^2 v}{\partial x^2} + w\frac{\partial^2 w}{\partial x^2}\right) + n_y^2\left(u\frac{\partial^2 u}{\partial y^2} + v\frac{\partial^2 v}{\partial y^2} + w\frac{\partial^2 w}{\partial y^2}\right)\right.$$

$$+ n_z^2\left(u\frac{\partial^2 u}{\partial z^2} + v\frac{\partial^2 v}{\partial z^2} + w\frac{\partial^2 w}{\partial z^2}\right) + 2n_x n_y\left(u\frac{\partial^2 v}{\partial x^2} + v\frac{\partial^2 u}{\partial y^2} + w\frac{\partial^2 w}{\partial x\partial y}\right)$$

$$\left. + 2n_x n_z\left(u\frac{\partial^2 w}{\partial x^2} + v\frac{\partial^2 w}{\partial x\partial y} + w\frac{\partial^2 u}{\partial z^2}\right) + 2n_y n_z\left(u\frac{\partial^2 w}{\partial x\partial y} + v\frac{\partial^2 w}{\partial y^2} + w\frac{\partial^2 v}{\partial z^2}\right)\right]$$

$$+ 4(\alpha_1 + \alpha_2)\left\{n_x^2\left[\left(\frac{\partial u}{\partial x}\right)^2 + \left(\frac{\partial v}{\partial x}\right)^2 + \left(\frac{\partial w}{\partial x}\right)^2\right] + n_y^2\left[\left(\frac{\partial v}{\partial x}\right)^2 + \left(\frac{\partial v}{\partial y}\right)^2 + \left(\frac{\partial v}{\partial z}\right)^2\right]\right.$$

$$+ n_z^2\left[\left(\frac{\partial w}{\partial x}\right)^2 + \left(\frac{\partial w}{\partial y}\right)^2 + \left(\frac{\partial w}{\partial z}\right)^2\right] + 2n_x n_y\left[\frac{\partial u}{\partial x}\frac{\partial v}{\partial x} + \frac{\partial v}{\partial x}\frac{\partial v}{\partial y} + \frac{\partial w}{\partial x}\frac{\partial w}{\partial y}\right]$$

$$+ 2n_x n_z\left[\frac{\partial u}{\partial x}\frac{\partial w}{\partial x} + \frac{\partial v}{\partial x}\frac{\partial w}{\partial y} + \frac{\partial w}{\partial x}\frac{\partial w}{\partial z}\right]$$

$$\left. + 2n_y n_z\left[\frac{\partial v}{\partial x}\frac{\partial w}{\partial x} + \frac{\partial v}{\partial y}\frac{\partial w}{\partial y} + \frac{\partial w}{\partial y}\frac{\partial w}{\partial z}\right]\right\}, \tag{5.5}$$

where

$$\frac{\partial^2 u}{\partial x^2} = \left(3\frac{\partial^2 \lambda}{\partial x^2} + x\frac{\partial^3 \lambda}{\partial x^3}\right)\frac{\partial \Gamma}{\partial \lambda} + 3\frac{\partial \lambda}{\partial x}\left(\frac{\partial \lambda}{\partial x} + x\frac{\partial^2 \lambda}{\partial x^2}\right)\frac{\partial^2 \Gamma}{\partial \lambda^2} + x\left(\frac{\partial \lambda}{\partial x}\right)^3\frac{\partial^3 \Gamma}{\partial \lambda^3},$$

$$\frac{\partial^2 v}{\partial x^2} = \left(2\frac{\partial^2 \lambda}{\partial x \partial y} + x\frac{\partial^3 \lambda}{\partial x^2 \partial y}\right)\frac{\partial \Gamma}{\partial \lambda} + \left(2\frac{\partial \lambda}{\partial x}\frac{\partial \lambda}{\partial y} + x\frac{\partial^2 \lambda}{\partial x^2}\frac{\partial \lambda}{\partial y} + 2x\frac{\partial \lambda}{\partial x}\frac{\partial^2 \lambda}{\partial x \partial y}\right)\frac{\partial^2 \Gamma}{\partial \lambda^2}$$

$$+ x\left(\frac{\partial \lambda}{\partial x}\right)^2\frac{\partial \lambda}{\partial y}\frac{\partial^3 \Gamma}{\partial \lambda^3},$$

$$\frac{\partial^2 w}{\partial x^2} = \left(2\frac{\partial^2 \lambda}{\partial x \partial z} + x\frac{\partial^3 \lambda}{\partial x^2 \partial z}\right)\frac{\partial \Gamma}{\partial \lambda} + \left(2\frac{\partial \lambda}{\partial x}\frac{\partial \lambda}{\partial z} + x\frac{\partial^2 \lambda}{\partial x^2}\frac{\partial \lambda}{\partial z} + 2x\frac{\partial \lambda}{\partial x}\frac{\partial^2 \lambda}{\partial x \partial z}\right)\frac{\partial^2 \Gamma}{\partial \lambda^2}$$

$$+ x\left(\frac{\partial \lambda}{\partial x}\right)^2\frac{\partial \lambda}{\partial z}\frac{\partial^3 \Gamma}{\partial \lambda^3},$$

$$\frac{\partial^2 u}{\partial y^2} = \left(\frac{\partial^2 \lambda}{\partial y^2} + x\frac{\partial^3 \lambda}{\partial x \partial y^2}\right)\frac{\partial \Gamma}{\partial \lambda} + \left(\left(\frac{\partial \lambda}{\partial y}\right)^2 + 2x\frac{\partial \lambda}{\partial y}\frac{\partial^2 \lambda}{\partial x \partial y} + x\frac{\partial \lambda}{\partial x}\frac{\partial^2 \lambda}{\partial y^2}\right)\frac{\partial^2 \Gamma}{\partial \lambda^2} + x\frac{\partial \lambda}{\partial x}\left(\frac{\partial \lambda}{\partial y}\right)^2\frac{\partial^3 \Gamma}{\partial \lambda^3},$$

$$\frac{\partial^2 v}{\partial y^2} = x\frac{\partial^3 \lambda}{\partial y^3}\frac{\partial \Gamma}{\partial \lambda} + 3x\frac{\partial \lambda}{\partial y}\frac{\partial^2 \lambda}{\partial y^2}\frac{\partial^2 \Gamma}{\partial \lambda^2} + x\left(\frac{\partial \lambda}{\partial y}\right)^3\frac{\partial^3 \Gamma}{\partial \lambda^3},$$

$$\frac{\partial^2 w}{\partial y^2} = x\frac{\partial^3 \lambda}{\partial y^2 \partial z}\frac{\partial \Gamma}{\partial \lambda} + \left(x\frac{\partial^2 \lambda}{\partial y^2}\frac{\partial \lambda}{\partial z} + 2x\frac{\partial \lambda}{\partial y}\frac{\partial^2 \lambda}{\partial y \partial z}\right)\frac{\partial^2 \Gamma}{\partial \lambda^2} + x\left(\frac{\partial \lambda}{\partial y}\right)^2\frac{\partial \lambda}{\partial z}\frac{\partial^3 \Gamma}{\partial \lambda^3},$$

$$\frac{\partial^2 u}{\partial z^2} = \left(\frac{\partial^2 \lambda}{\partial z^2} + x\frac{\partial^3 \lambda}{\partial x \partial z^2}\right)\frac{\partial \Gamma}{\partial \lambda} + \left(\left(\frac{\partial \lambda}{\partial z}\right)^2 + 2x\frac{\partial^2 \lambda}{\partial x \partial z}\frac{\partial \lambda}{\partial z} + x\frac{\partial \lambda}{\partial x}\frac{\partial^2 \lambda}{\partial z^2}\right)\frac{\partial^2 \Gamma}{\partial \lambda^2} + x\frac{\partial \lambda}{\partial x}\left(\frac{\partial \lambda}{\partial z}\right)^2\frac{\partial^3 \Gamma}{\partial \lambda^3},$$

$$\frac{\partial^2 v}{\partial z^2} = x\frac{\partial^3 \lambda}{\partial y \partial z^2}\frac{\partial \Gamma}{\partial \lambda} + \left(2x\frac{\partial \lambda}{\partial z}\frac{\partial^2 \lambda}{\partial y \partial z} + x\frac{\partial \lambda}{\partial y}\frac{\partial^2 \lambda}{\partial z^2}\right)\frac{\partial^2 \Gamma}{\partial \lambda^2} + x\frac{\partial \lambda}{\partial y}\left(\frac{\partial \lambda}{\partial z}\right)^2\frac{\partial^3 \Gamma}{\partial \lambda^3},$$

$$\frac{\partial^2 w}{\partial z^2} = x\frac{\partial^3 \lambda}{\partial z^3}\frac{\partial \Gamma}{\partial \lambda} + 3x\frac{\partial \lambda}{\partial z}\frac{\partial^2 \lambda}{\partial z^2}\frac{\partial^2 \Gamma}{\partial \lambda^2} + x\left(\frac{\partial \lambda}{\partial z}\right)^3\frac{\partial^3 \Gamma}{\partial \lambda^3},$$

$$\frac{\partial^2 w}{\partial x \partial y} = \left(\frac{\partial^2 \lambda}{\partial y \partial z} + x\frac{\partial^3 \lambda}{\partial x \partial y \partial z}\right)\frac{\partial \Gamma}{\partial \lambda} + \left(\frac{\partial \lambda}{\partial y}\frac{\partial \lambda}{\partial z} + x\frac{\partial \lambda}{\partial z}\frac{\partial^2 \lambda}{\partial x \partial y} + x\frac{\partial \lambda}{\partial x}\frac{\partial^2 \lambda}{\partial y \partial z} + x\frac{\partial \lambda}{\partial y}\frac{\partial^2 \lambda}{\partial x \partial z}\right)\frac{\partial^2 \Gamma}{\partial \lambda^2}$$

$$+ x\frac{\partial \lambda}{\partial x}\frac{\partial \lambda}{\partial y}\frac{\partial \lambda}{\partial z}\frac{\partial^3 \Gamma}{\partial \lambda^3}.$$

$$(5.6)$$

The higher order derivatives of the ellipsoidal parameter $\lambda$, are obtained from the first derivatives given by (3.10) with $\lambda = \lambda(x, y, z)$.

With $u$, $v$, and $w$ given by (3.28), the resulting normal stress for a second-order fluid around an ellipsoid is of the form $T_{nn} = T_{nn}(x, y, z, \lambda)$. On the surface of the ellipsoid $\lambda = 0$, so that the normal component of the stress on the surface of the ellipsoid is a function of the Cartesian coordinates only. The dimensionless form of the normal stress
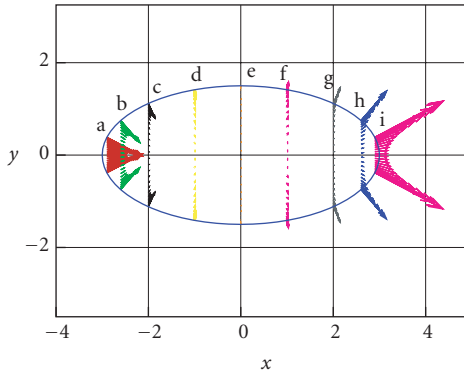
Figure 6.1. Distribution of the normal stress at the surface of a tri-axial ellipsoid, immersed in a uniform stream that moves from left to right. Two-dimensional representation in the $(x, y)$-plane of an ellipsoid (with semiaxes $a = 3$, $b = 1.5$, $c = 0.75$ cm). The arrows represent the normal stress $(T_{nn}n_x + T_{nn}n_y)/150$ dyn/cm$^2$ evaluated for different cross sections along the ellipsoid. The cross sections are located at (a) $x = -2.9$, (b) $-2.6$, (c) $-2.0$, (d) $-1.0$, (e) $0.0$, (f) $1.0$, (g) $2.0$, (h) $2.6$, and (i) $2.9$ cm. A perpendicular view of the different cross sections is shown in Figures 6.2–6.10. There is compression in the fore part of the ellipsoid and a strong tension in the rear, near the trailing stagnation point.

at the surface is expressed as

$$T_{nn}^* = \frac{T_{nn} + p_\infty}{\rho U^2/2}.$$
(5.7)

## 6. Normal stress distribution on the ellipsoid

Here we present the results of the normal stress evaluated at the surface of an ellipsoid, immersed in a uniform flow of a second-order fluid, for a Reynolds number (Re = $\rho U a/\eta$) of 0.05. Three different cases are shown to illustrate the effects of the semiaxes ratios in the stress distribution. First, the normal stress is evaluated on a tri-axial ellipsoid with $a/b = b/c = 2$. The second case corresponds to a flatter ellipsoid with $a/b = 2$ and $b/c = 5$. Finally, we show the distribution of the stress at the surface of a prolate spheroid with $a/b = 2$ and $b = c$. As an example of second-order fluid we used the liquid M1 with the following properties (Hu et al. [3]): [$\rho = 0.895$ g/cm$^3$, $\eta = 30$ P, $\alpha_1 = -3$, and $\alpha_2 = 5.34$ g/cm].

The distribution and sign of the normal stress at the surface is depicted by arrows around ellipses that represent cross sections of the ellipsoid (see Figures 6.1, 6.2, 6.3, 6.4, 6.5, 6.6, 6.7, 6.8, 6.9, 6.10, 6.11, and 6.12). If the normal stress is negative it gives rise to compression and if positive, it induces tensions that may be responsible for the deformation of gas bubbles in viscoelastic liquids. Inward arrows represent the negative values and outward arrows represent the positive values of the normal stress. We also present the results of the dimensionless normal stress $T_{nn}^*$, as a function of the polar angle $\theta$ (see Figures 6.13 and 6.14).
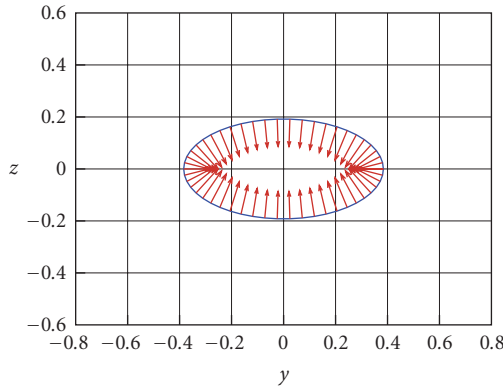
Figure 6.2. Normal stress $(T_{nn}n_y + T_{nn}n_z)/600\,\mathrm{dyn/cm^2}$ for an ellipse $y^2/b^2 + z^2/c^2 = 1 - 2.9^2/a^2$ at $x = -2.9\,\mathrm{cm}$ in the $(y,z)$-plane. Perpendicular view of the cross section (a) in Figure 6.1. The normal stress at the front of the ellipsoid gives rise to compression near the leading edge. This may explain the flat top observed in gas bubbles rising in viscoelastic fluids (see Figure 2.1).
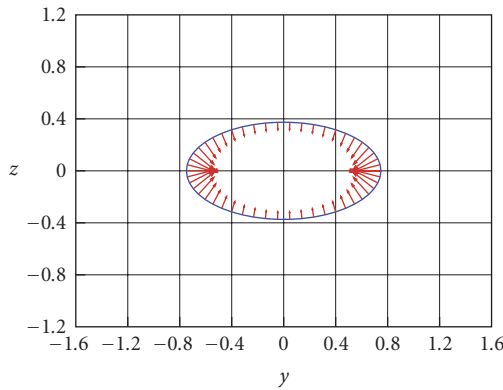


Figure 6.3. Normal stress $(T_{nn}n_y + T_{nn}n_z)/300\,\mathrm{dyn/cm^2}$ for an ellipse $y^2/b^2 + z^2/c^2 = 1 - 2.6^2/a^2$ at $x = -2.6\,\mathrm{cm}$ in the $(y,z)$-plane. Perpendicular view of the cross section (b) in Figure 6.1. There is a bigger compression (indicated by bigger inwards arrows) at the right and left poles of the ellipse. This may cause that the cross section of the ellipsoid becomes more round and in consequence the ellipsoid would tend to be prolate.

The normal stress distribution on the surface of a tri-axial ellipsoid with $a = 3$, $b = 1.5$, and $c = 0.75\,\mathrm{cm}$, shown in Figures 6.1–6.10, suggest the formation of a gas bubble with a prolate shape in the front and a flat two-dimensional shape in the back with an elongated trailing edge.

We made the former ellipsoid even flatter by making $c = 0.3\,\mathrm{cm}$. The computed normal stress distribution is depicted in Figure 6.11. The results indicate that as the rear part
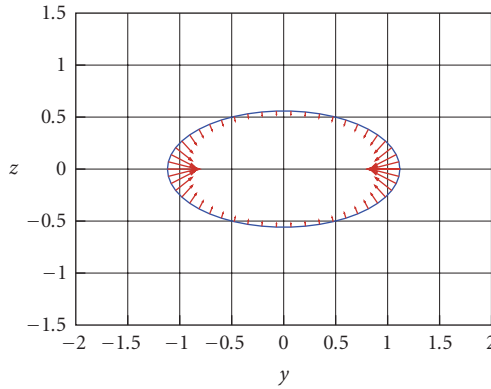
Figure 6.4. Normal stress $(T_{nn}n_y + T_{nn}n_z)/150$ dyn/cm$^2$ for an ellipse $y^2/b^2 + z^2/c^2 = 1 - 2.0^2/a^2$ at $x = -2.0$ cm in the $(y,z)$-plane. Perpendicular view of the cross section (c) in **Figure 6.1**. Strong compression at the right and left poles of the ellipse and mild compression towards the center.
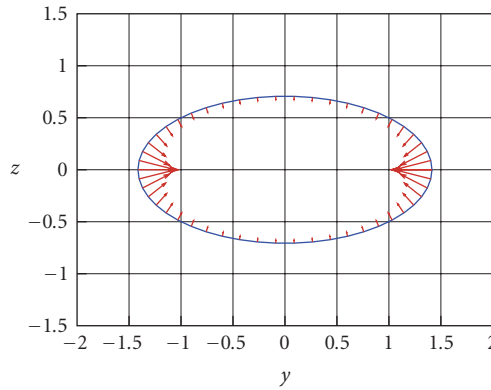


Figure 6.5. Normal stress $(T_{nn}n_y + T_{nn}n_z)/50$ dyn/cm$^2$ for an ellipse $y^2/b^2 + z^2/c^2 = 1 - 1.0^2/a^2$ at $x = -1.0$ cm in the $(y,z)$-plane. Perpendicular view of the cross section (d) in **Figure 6.1**. Small compression at the center and high compression at the right and left poles of the ellipse (indicated by small and big inwards arrows). This suggests that the upper part of a gas bubble rising in a viscoelastic fluid would tend to be prolate.

of the bubble gets flatter, the pulling out effect at the right and left poles increase giving rise to a thinner tail.

Once the bubble acquires the prolate shape in the front, the stresses around the ellipsoid become constant for each cross section. This is shown in **Figure 6.12**, that represent the stresses around the ellipsoid with $a = 3.0$, $b = 1.5$, and $c = 1.5$ cm. The normal stress for each cross section located at: $x = -2.9, -2.6, -2.0, -1.0, 0.0, 1.0, 2.0, 2.6,$ and $2.9$, is constant and they are all compression in the front and tension in the back. For the three
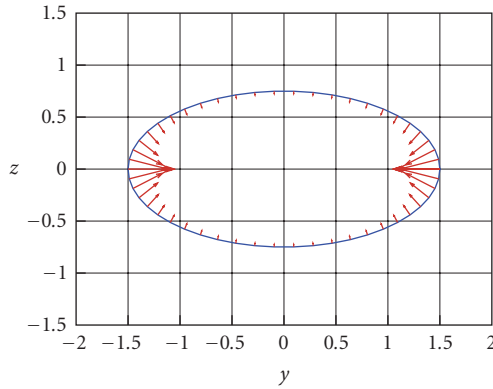
Figure 6.6. Normal stress $(T_{nn}n_y + T_{nn}n_z)/2.5$ dyn/cm$^2$ for an ellipse $y^2/b^2 + z^2/c^2 = 1$ at $x = 0.0$ cm in the $(y,z)$-plane. Perpendicular view of the cross section (e) in **Figure 6.1**. There is still compression right in the middle of the ellipsoid.
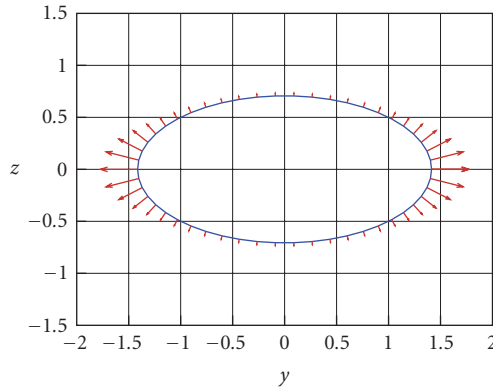


Figure 6.7. Normal stress $(T_{nn}n_y + T_{nn}n_z)/50$ dyn/cm$^2$ for an ellipse $y^2/b^2 + z^2/c^2 = 1 - 1.0^2/a^2$ at $x = 1.0$ cm in the $(y,z)$-plane. Perpendicular view of the cross section (f) in **Figure 6.1**. There is a change of sign of the normal stress right after the front half of the ellipsoid. It changes from negative (compression) to positive (tension). Strong tension near the right and left poles and mild tension towards the center. This may induce the formation of a flat tail for a gas bubble. The same effect is observed in the other cross sections of the rear part of the ellipsoid (see Figures 6.8–6.10).

semiaxes ratios covered in this study, there is a strong tension near the rear stagnation point that could be responsible for the build up of a two-dimensional cusp at the trailing edge of a bubble.

   **Figure 6.13** shows a maximum compression near the leading edge. The maximum tension, that is almost twice the maximum compression, is located very close to the trailing edge (see **Figure 6.14**).
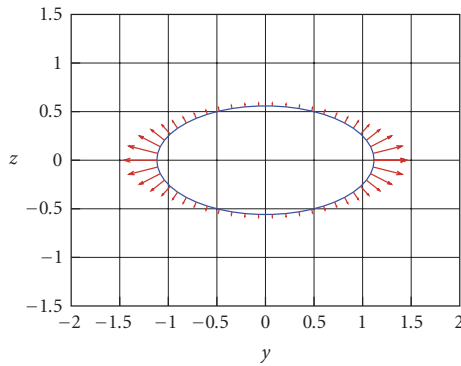
Figure 6.8. Normal stress $(T_{nn}n_y + T_{nn}n_z)/150 \, \mathrm{dyn/cm^2}$ for an ellipse $y^2/b^2 + z^2/c^2 = 1 - 2.0^2/a^2$ at $x = 2.0 \, \mathrm{cm}$ in the $(y,z)$-plane. Perpendicular view of the cross section (g) in **Figure 6.1**. Strong tension at the right and left poles causes the ellipsoid to get flatter.
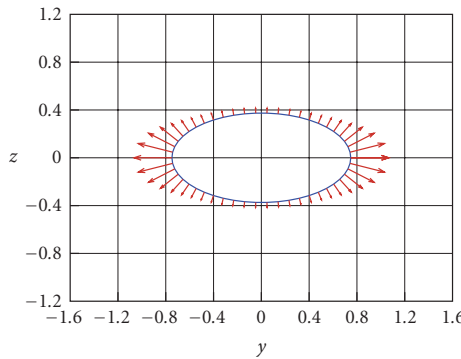


Figure 6.9. Normal stress $(T_{nn}n_y + T_{nn}n_z)/300 \, \mathrm{dyn/cm^2}$ for an ellipse $y^2/b^2 + z^2/c^2 = 1 - 2.6^2/a^2$ at $x = 2.6 \, \mathrm{cm}$ in the $(y,z)$-plane. Perpendicular view of the cross section (h) in **Figure 6.1**. Strong tension at the right and left poles causes the ellipsoid to get flatter.
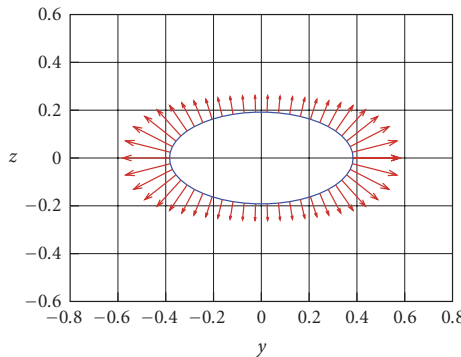


Figure 6.10. Normal stress $(T_{nn}n_y + T_{nn}n_z)/600 \, \mathrm{dyn/cm^2}$ for an ellipse $y^2/b^2 + z^2/c^2 = 1 - 2.9^2/a^2$ at $x = 2.9 \, \mathrm{cm}$ in the $(y,z)$-plane. Perpendicular view of the cross section (i) in **Figure 6.1**. The strong tension observed near the trailing stagnation point may explain the formation of a two-dimensional cusping tail in a gas bubble rising in viscoelastic fluids.
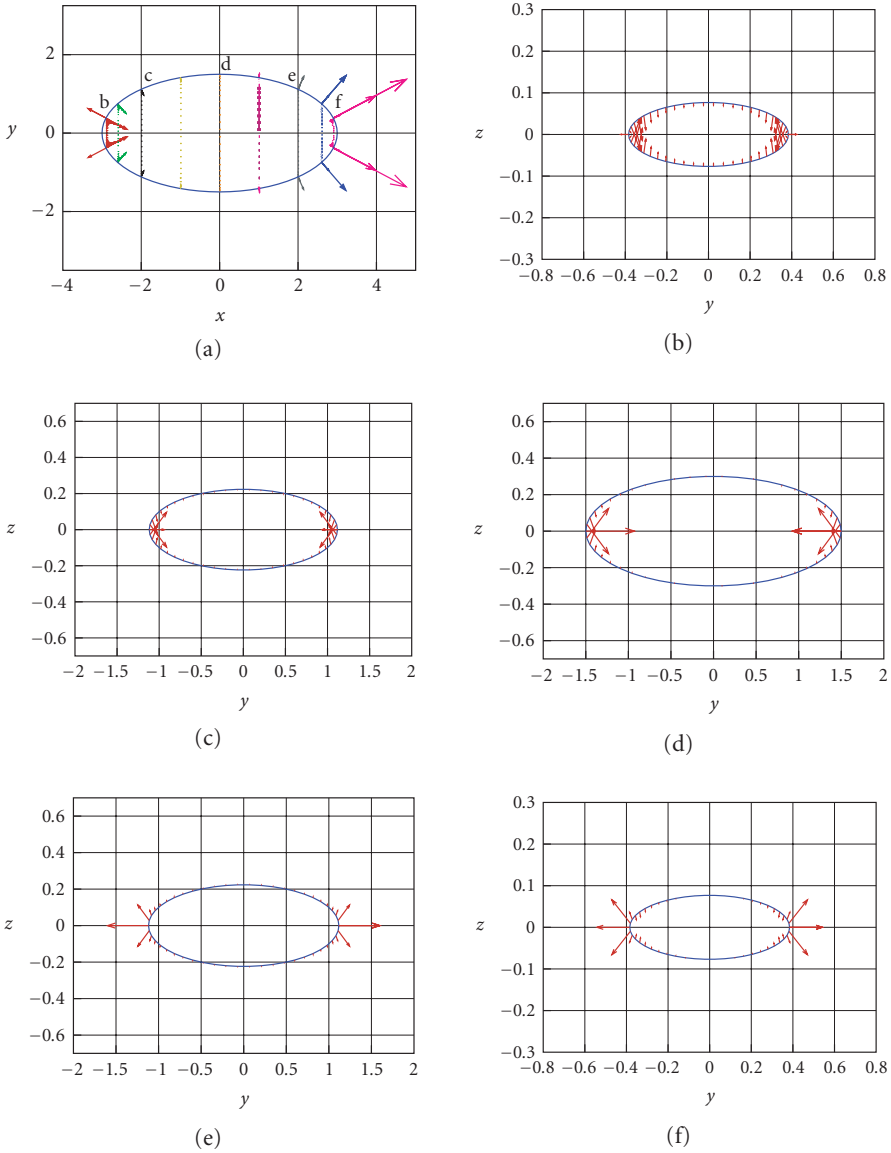
Figure 6.11. Distribution of the normal stress $T_{nn}$ on various cross sections on the $(y,z)$-planes of an ellipsoid (with semiaxes $a = 3$, $b = 1.5$, $c = 0.3$ cm) immerse in a flow of fluid M1 (moving from left to right) with a Reynolds number of 0.05. (a) $(T_{nn}n_x + T_{nn}n_y)/1200$ dyn/cm² for an ellipsoid $x^2/a^2 + y^2/b^2 = 1 - z^2/c^2$ with $z = 0$, in the $(x,y)$-plane. (b) $(T_{nn}n_y + T_{nn}n_z)/7500$ dyn/cm² for an ellipsoid $y^2/b^2 + z^2/c^2 = 1 - x^2/a^2$ with $x = -2.9$ cm, in the $(y,z)$-plane. (c) $(T_{nn}n_y + T_{nn}n_z)/800$ dyn/cm² for an ellipsoid $y^2/b^2 + z^2/c^2 = 1 - x^2/a^2$ with $x = -2.0$ cm, in the $(y,z)$-plane. (d) $(T_{nn}n_y + T_{nn}n_z)/10$ dyn/cm² for an ellipsoid $y^2/b^2 + z^2/c^2 = 1 - x^2/a^2$ with $x = 0.0$ cm, in the $(y,z)$-plane. (e) $(T_{nn}n_y + T_{nn}n_z)/800$ dyn/cm² for an ellipsoid $y^2/b^2 + z^2/c^2 = 1 - x^2/a^2$ with $x = 2.0$ cm, in the $(y,z)$-plane. (f) $(T_{nn}n_y + T_{nn}n_z)/7500$ dyn/cm² for an ellipsoid $y^2/b^2 + z^2/c^2 = 1 - x^2/a^2$ with $x = 2.9$ cm, in the $(y,z)$-plane.
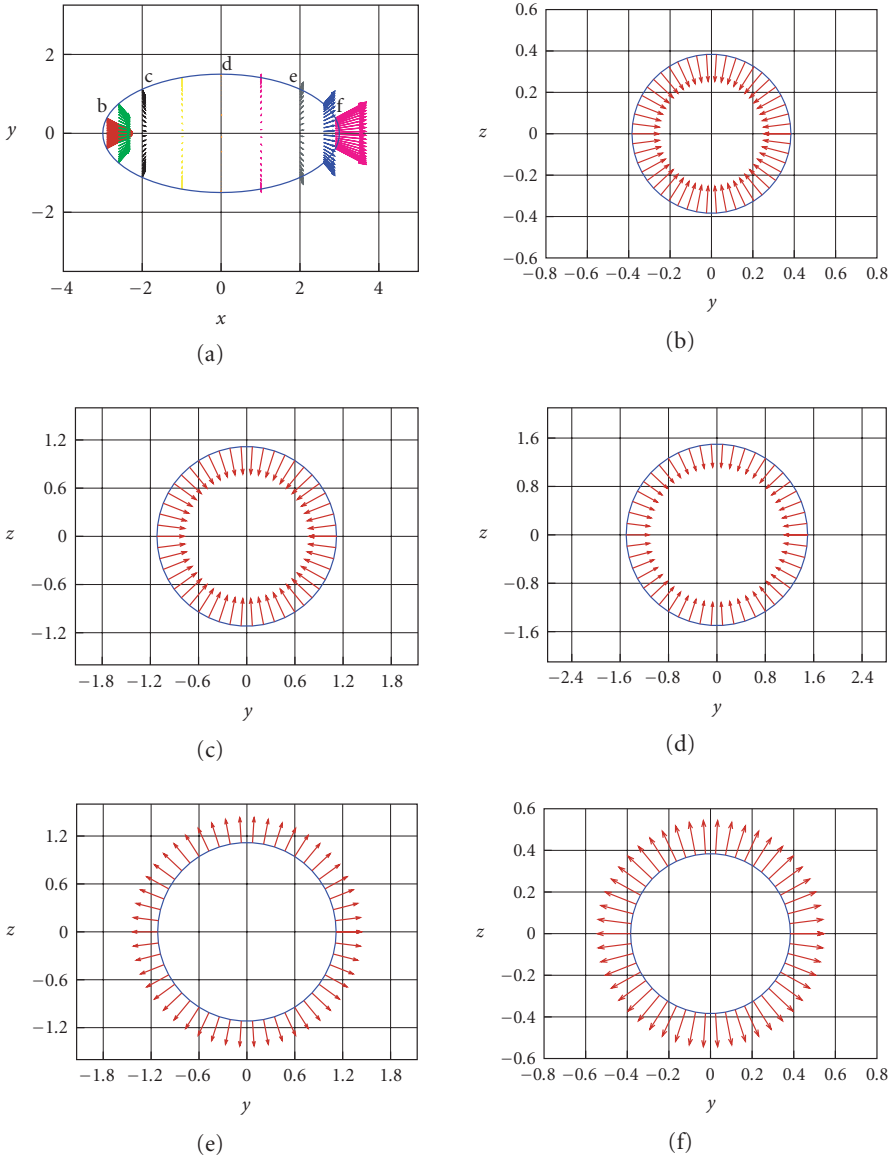
Figure 6.12. Distribution of the normal stress $T_{nn}$ on various cross sections on the $(y, z)$-planes of an ellipsoid (with semiaxes $a = 3$, $b = 1.5$, $c = 1.5$ cm) immerse in a flow of fluid M1 with a Reynolds number of 0.05. (a) $(T_{nn}n_x + T_{nn}n_y)/100$ dyn/cm² for an ellipsoid $x^2/a^2 + y^2/b^2 = 1 - z^2/c^2$ with $z = 0$, in the $(x, y)$-plane. (b) $(T_{nn}n_y + T_{nn}n_z)/250$ dyn/cm² for an ellipsoid $y^2/b^2 + z^2/c^2 = 1 - x^2/a^2$ with $x = -2.9$ cm, in the $(y, z)$-plane. (c) $(T_{nn}n_y + T_{nn}n_z)/50$ dyn/cm² for an ellipsoid $y^2/b^2 + z^2/c^2 = 1 - x^2/a^2$ with $x = -2.0$ cm, in the $(y, z)$-plane. (d) $(T_{nn}n_y + T_{nn}n_z)$ dyn/cm² for an ellipsoid $y^2/b^2 + z^2/c^2 = 1 - x^2/a^2$ with $x = 0.0$ cm, in the $(y, z)$-plane. (e) $(T_{nn}n_y + T_{nn}n_z)/50$ dyn/cm² for an ellipsoid $y^2/b^2 + z^2/c^2 = 1 - x^2/a^2$ with $x = 2.0$ cm, in the $(y, z)$-plane. (f) $(T_{nn}n_y + T_{nn}n_z)/250$ dyn/cm² for an ellipsoid $y^2/b^2 + z^2/c^2 = 1 - x^2/a^2$ with $x = 2.9$ cm, in the $(y, z)$-plane.
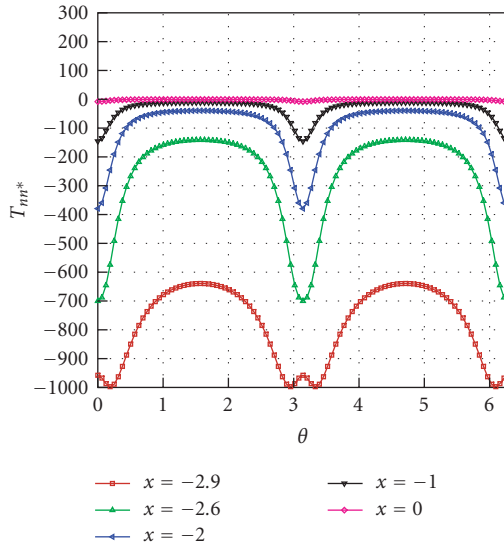
Figure 6.13. Dimensionless normal stress as a function of the polar angle $\theta$ for the different cross sections of the frontal part of the ellipsoid shown in Figures 6.2–6.6 ($x \leq 0$). The normal stress is compression in the fore part of the ellipsoid. The maximum compression is observed near the leading edge and decreases as we move towards the rear of the ellipsoid.
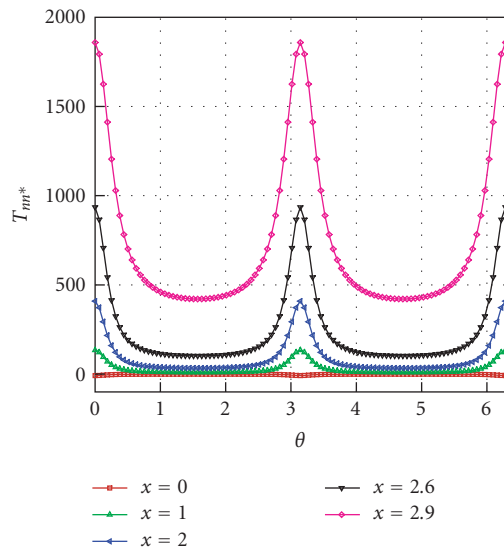


Figure 6.14. Dimensionless normal stress as a function of the polar angle $\theta$ for the different cross sections of the rear part of the ellipsoid shown in Figures 6.6–6.10 ($x \geq 0$). The normal stress is tension in the rear of the ellipsoid, with a strong tension near the trailing edge.

## 7. Conclusions

We developed the analysis of viscoelastic potential flow of a second-order fluid around an ellipsoid. To carry out these calculations we formed expressions for the velocity, the inviscid pressure, the velocity derivatives and the composition of these derivatives to compute stresses. The calculations give rise to normal stress distribution compatible with experimental observations of gas bubbles rising in viscoelastic liquids. In particular, the normal stress at the top of a rising bubble is compression and the side stress tends to round the elliptic shape. The trailing edge of the bubble is stretched into a cusp and the side of the ellipse tends to flatten into the remarkable two-dimensional cusps observed in experiments. Since the velocity is obtained from a harmonic potential, the velocity field does not depend on viscous or viscoelastic parameters. This suggests that the cusping effect is associated primarily with normal stresses rather than with secondary effects due to changes in velocity not computed here.

## References

[1]   P. F. Byrd and M. D. Friedman, *Handbook of Elliptic Integrals for Engineers and Scientists*, 2nd ed., Die Grundlehren der mathematischen Wissenschaften, vol. 67, Springer, New York, 1971.

[2]   O. Hassager, *Negative wake behind bubbles in non-Newtonian liquids*, Nature **279** (1979), 402–403.

[3]   H. H. Hu, O. Riccius, K. P. Chen, M. Arney, and D. D. Joseph, *Climbing constant, second-order correction of Trouton's viscosity, wave speed and delayed die swell for M1*, J. Non-Newtonian Fluid Mech. **35** (1990), no. 2-3, 287–307.

[4]   D. D. Joseph, *Bernoulli equation and the competition of elastic and inertial pressures in the potential flow of a second-order fluid*, J. Non-Newtonian Fluid Mech. **42** (1992), no. 3, 385–389.

[5]   ———, *Understanding cusped interfaces*, J. Non-Newtonian Fluid Mech. **44** (1992), 127–148.

[6]   ———, *Flow induced microstructure in newtonian and viscoelastic fluids*, Proceedings of the 5th World Congress of Chemical Engineering, Particle Technology Track (San Diego, 1996), Second Particle Technology, vol. 6, American Institute of Chemical Engineers, New York, 1996, pp. 3–16.

[7]   D. D. Joseph and J. Feng, *A note on the forces that move particles in a second-order fluid*, J. Non-Newtonian Fluid Mech. **64** (1996), no. 2-3, 299–302.

[8]   D. D. Joseph, J. Nelson, M. Renardy, and Y. Renardy, *Two-dimensional cusped interfaces*, J. Fluid Mech. **223** (1991), 383–409.

[9]   O. D. Kellogg, *Foundations of Potential Theory*, Dover, New York, 1929.

[10]  H. Lamb, *Hydrodynamics*, 6th ed., Cambridge Mathematical Library, Cambridge University Press, Cambridge, 1993.

[11]  Y. J. Liu, T. Y. Liao, and D. D. Joseph, *A two-dimensional cusp at the trailing edge of an air bubble rising in a viscoelastic liquid*, J. Fluid Mech. **304** (1995), 321–342.

[12]  L. M. Milne-Thomson, *Theoretical Hydrodynamics*, 5th ed., Dover, New York, 1996.

[13]  S. B. Pillapakkam and P. Singh, *A level-set method for computing solutions to viscoelastic two-phase flow*, J. Comput. Phys. **174** (2001), no. 2, 552–578.

[14]  ———, *Negative wake and velocity of a bubble rising in a viscoelastic fluid*, Proceedings of the ASME International Mechanical Engineering Congress & RD&D Expo (Washington, DC, 2003), Fluids Engineering Division, vol. 259, American Society of Mechanical Engineers, New York, 2003, pp. 709–714.

[15]    J. Wang and D. D. Joseph, *Potential flow of a second-order fluid over a sphere or an ellipse*, J. Fluid
        Mech. **511** (2004), 201–215.

F. Viana: Department of Aerospace Engineering and Mechanics, University of Minnesota, 110
Union Street SE, Minneapolis, MN 55455, USA
    *E-mail address*: vianaf@aem.umn.edu

T. Funada: Department of Digital Engineering, Numazu National College of Technology, 3600
Ooka, Numazu-shi, Shizuoka 410-8501, Japan
    *E-mail address*: funada@ece.numazu-ct.ac.jp

D. D. Joseph: Department of Aerospace Engineering and Mechanics, University of Minnesota, 110
Union Street SE, Minneapolis, MN 55455, USA
    *E-mail address*: joseph@aem.umn.edu

N. Tashiro: Department of Digital Engineering, Numazu National College of Technology, 3600
Ooka, Numazu-shi, Shizuoka 410-8501, Japan
    *E-mail address*: naoto@eces.numazu-ct-ac.jp

Y. Sonoda: Department of Digital Engineering, Numazu National College of Technology, 3600
Ooka, Numazu-shi, Shizuoka 410-8501, Japan
    *E-mail address*: sonoda@eces.numazu-ct.ac.jp

# Special Issue on Time-Dependent Billiards

## Call for Papers

This subject has been extensively studied in the past years for one-, two-, and three-dimensional space. Additionally, such dynamical systems can exhibit a very important and still unexplained phenomenon, called as the Fermi acceleration phenomenon. Basically, the phenomenon of Fermi acceleration (FA) is a process in which a classical particle can acquire unbounded energy from collisions with a heavy moving wall. This phenomenon was originally proposed by Enrico Fermi in 1949 as a possible explanation of the origin of the large energies of the cosmic particles. His original model was then modified and considered under different approaches and using many versions. Moreover, applications of FA have been of a large broad interest in many different fields of science including plasma physics, astrophysics, atomic physics, optics, and time-dependent billiard problems and they are useful for controlling chaos in Engineering and dynamical systems exhibiting chaos (both conservative and dissipative chaos).

We intend to publish in this special issue papers reporting research on time-dependent billiards. The topic includes both conservative and dissipative dynamics. Papers discussing dynamical properties, statistical and mathematical results, stability investigation of the phase space structure, the phenomenon of Fermi acceleration, conditions for having suppression of Fermi acceleration, and computational and numerical methods for exploring these structures and applications are welcome.

To be acceptable for publication in the special issue of Mathematical Problems in Engineering, papers must make significant, original, and correct contributions to one or more of the topics above mentioned. Mathematical papers regarding the topics above are also welcome.

Authors should follow the Mathematical Problems in Engineering manuscript format described at http://www.hindawi.com/journals/mpe/. Prospective authors should submit an electronic copy of their complete manuscript through the journal Manuscript Tracking System at http://mts.hindawi.com/ according to the following timetable:

| Manuscript Due | March 1, 2009 |
| --- | --- |
| First Round of Reviews | June 1, 2009 |
| Publication Date | September 1, 2009 |

**Guest Editors**

**Edson Denis Leonel,** Department of Statistics, Applied Mathematics and Computing, Institute of Geosciences and Exact Sciences, State University of São Paulo at Rio Claro, Avenida 24A, 1515 Bela Vista, 13506-700 Rio Claro, SP, Brazil; edleonel@rc.unesp.br

**Alexander Loskutov,** Physics Faculty, Moscow State University, Vorob'evy Gory, Moscow 119992, Russia; loskutov@chaos.phys.msu.ru